TOWARDS A NEW UNDERSTANDING OF FATIGUE CRACK PROPAGATION

D. Nowell[1,2*], P. Qui[2]

[1]Department of Mechanical Engineering, Imperial College London
South Kensington Campus, London SW7 2AZ, UK.
[2]Department of Engineering Science, University of Oxford, Parks Road, Oxford, OX1 3PJ, UK.
[*] Persona de contacto: d.nowell@imperial.ac.uk

RESUMEN

La propagación de grietas por fatiga ocupa gran parte de la vida de los componentes de ingeniería, particularmente en el régimen de grietas cortas. Es importante comprender los mecanismos de propagación para llevar a cabo la evaluación de la tolerancia al daño y para predecir la vida útil de los componentes. Este artículo describe experimentos llevados a cabo en las escalas macro y micro, utilizando la técnica de correlación de imágenes digitales para medir desplazamientos cercanos al vértice de la grieta. A partir de estos desplazamientos se pueden extraer varios parámetros clave que rigen el crecimiento de grietas, y se pueden validar diferentes modelos de deformación de grietas por fatiga. El documento describe toda la metodología y analiza los requisitos para futuras investigaciones dirigidas a una mejor comprensión del crecimiento de grietas por fatiga.

PALABRAS CLAVE: Fatiga, Blindaje de punta de grieta, Correlación de imagen digital

ABSTRACT

Fatigue crack propagation occupies much of the life of engineering components, particularly in the short crack regime. It is important to understand the mechanisms of propagation in order to carry out damage tolerance assessment and to predict component service life. The paper describes experiments carried out at macro- and micro-scale using digital image correlation to measure near-tip displacements. From these, various key parameters governing crack growth may be extracted, and different models of fatigue crack deformation may be validated. The paper describes these, and discusses the requirements for future research aimed at an improved understanding of fatigue crack growth.

KEYWORDS: Fatigue, Crack tip shielding, Digital Image Correlation

INTRODUCTION

There is increasing pressure on designers to reduce the level of conservatism in engineering systems in order to meet targets on cost, weight and emissions. Most components suffer some form of cyclic stress, either directly from the remote loading (e.g. wind, or waves), or from vibrations originating within the system itself. It is therefore not surprising that the most common cause of failure in service is fatigue [1]. The 'safe life' approach to fatigue has been used for many years, but inherently the scatted in crack nucleation life results in excessive conservatism together with an acceptance of a small number of service failures. Hence, for high-value or safety critical components (such as disks in aero-engines or reactor components) the 'damage tolerant' approach is used, which relies on a combination of non-destructive inspection and estimation of crack propagation life. Most methods of this type are based on Paris and Erdogan's classic paper of 1963 [2], which relates crack growth rate to the range of stress intensity experienced by the crack tip:

$$\frac{da}{dN} = A\Delta K^n \tag{1}$$

Of course, the so-called Paris law is simply an empirical curve fit to experimental data, which is valid for constant amplitude loading at a single load ratio. Because it has proved so useful, various attempts have been made to extend the Paris law to more general conditions. Useful physical bases for this have been provided by Elber's 1970 observation of plasticity induced fatigue crack closure [3], and by the two parameter approach to crack growth characterisation [4]. However, neither of these have proved completely satisfactory. In any case, it is observed that cracks behave differently in the short crack regime than they do for microstructure independent growth. Hence, the stress intensity approach has significant limitations when applied to practical industrial problems. Recent advances in experimental techniques, coupled with improved numerical modelling approaches, mean that a pathway towards a new paradigm for fatigue crack growth modelling may now be apparent. This paper will summarise some recent

experimental work, and will suggest potential avenues for future exploration in order to produce more accurate management of service life in engineering systems.

EXPERIMENTS

Our original experimental approach to investigate fatigue crack closure involved the application of moiré interferometry. This method proved effective and yielded valuable results, however the experiments themselves were difficult and time consuming. More recently, de Matos pioneered the use of digital image correlation to investigate deformations close to a fatigue crack tip. This technique has been adopted by others, and a range of useful results are now available in the literature. Our own experiments have followed on from those of de Matos [5], and a typical experimental configuration is shown in Figure 1. A long-range microscope is used to collect the images with the aid of a digital camera. This enables data from close to the crack tip to be obtained. A typical image collected in this manner is shown in Figure 2 [6]. At the relatively large magnification employed, the machining marks on the surface of the specimen provided sufficient contrast to be used for feature recognition in the DIC algorithm. No painting of the surface is required. Whilst a number of commercial DIC codes are available, public domain software proves entirely acceptable for image analysis.

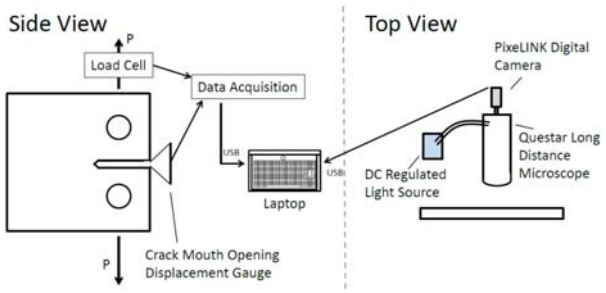

Figure 1. Schematic the experimental setup

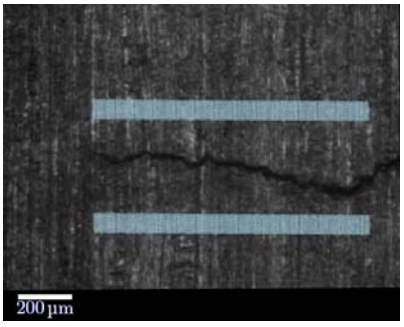

Figure 2. A typical image of a crack with a grid of points where displacements are measured using DIC (from [6])

As will be shown below, linear elastic fracture mechanics provides a reasonably good fit to measured surface displacements at this length scale. It is therefore interesting to investigate whether the same can be said for displacements measured much closer to the tip. A similar experimental procedure was therefore carried out using in situ loading in a scanning electron microscope [7]. Once again, DIC proved effective in determining the near tip displacements. A typical image collected in the microscope is shown in Figure 3. It will be seen that the field of view is about ten times smaller than that shown in Figure 2.

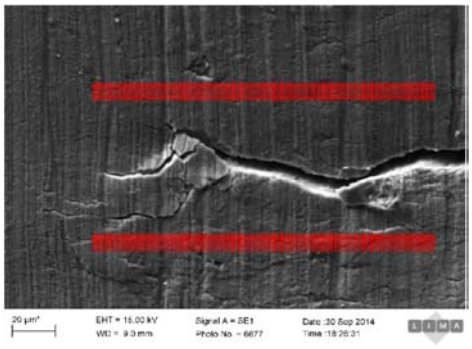

Figure 3. A typical image of a crack with obtained with a scanning electron microscope (from [6])

A number of authors have used the entire image to fit to various models for near tip displacement [7;8], but we should note that, since the crack is loaded in mode 1, the largest displacements are those in the y-direction along the crack flanks. Therefore, points close to the crack flanks contain the most information about the overall displacement, and as we will see in the next section, excellent results may be obtained using the relative displacement of pairs of points on either side of the crack [5].

CRACK TIP DISPLACEMENT FIELDS

The simplest crack tip field that can be envisaged is the elastic field for a sharp crack [9], but it is clear that a propagating fatigue crack differs from this in a number of respects. Ahead of the crack tip, there is a forward plastic zone, which may lead to significant crack tip blunting. There is also a cyclic plastic zone, which is approximately ¼ the size of the forward zone and where material undergoes cyclic plasticity as the crack is loaded. As the crack propagates through these zones, a plastic wake will develop, and arguments of self-similarity suggest that the strength of this will increase linearly with crack length. Finally, some closure may be present, which will cause the crack tip to be unloaded during part of the remote loading cycle. Various models have been suggested to account for some or all of these effects, but here we will concentrate on two: (i) The Pommier and Hamam Model [10] which takes some account of crack tip plasticity in a simplified form, and (ii) the more complex Christopher, James and Patterson model [11]. Before looking at these, however, we will compare our experimental results with the predictions of the simple elastic model.

2.1. The elastic crack tip field

The Westergaard stress function approach leads to a general expression for the displacement in Mode 1 loading, perpendicular to the crack path as

$$u_y = 2\frac{K}{E}\sqrt{\frac{r}{2\pi}}\sin\frac{\theta}{2}\left(1+\sin^2\frac{\theta}{2}-\nu\cos^2\frac{\theta}{2}\right) \quad (2)$$

where r is the radial distance from the crack tip, and θ is the polar angle measured from the extension of the crack path ahead of the tip. From this, by taking $\theta = \pm\pi$ one obtains an expression for the relative displacement between pairs of points on either side of the crack:

$$u_y = \frac{8K_I}{E}\sqrt{\frac{r}{2\pi}} \quad (3)$$

From this it is clear that the elastic model predicts that this displacement component should vary with distance from the crack as $\sqrt{r}$ and a plot of the experimentally displacement against $\sqrt{r}$ will give a value for the stress intensity factor, K, from the slope of the best fit straight line, provided that the Young's Modulus, E is known. The straightness of the line will give an indication of the appropriateness of the model. Alternatively, plotting $u_y/\sqrt{r}$ against r will give lines which are horizontal, and the stress intensity factor may be obtained from the intercept. Before doing this, however, we should note that as the points at which the displacement data is being measured (shown as the light blue grid in Figure 2) approach the crack tip, the approximation that $\theta = \pm\pi$ is no longer valid, and the full expression in equation (2) should be used, rather than that in equation (3). Figure 4 shows some typical data [sam] from a crack growing under constant amplitude cyclic loading. In Figure 4a, the approximation in equation (3) is used to fit the experimental data, whereas in Figure 4b, the full expression is used. It will be seen that a better fit is obtained using equation (2), which accommodates the non-zero experimental results corresponding to the crack tip position.

Figure 5 shows the results plotted according to the normalisation suggested above. It will be seen that the intercept with the vertical axis increases as the load is increased. From this data one can obtain a plot of stress intensity factor, K, against applied load $P/P_{max.}$ The corresponding graph is shown in Figure 6. When compared with the theoretical elastic stress intensity factor for the compact tension specimen geometry used, it can be seen that the slope of the line is similar, but there is an offset caused by some form of crack tip shielding. Hence, the stress intensity factor does not start to increase until a certain threshold load is reached. The most likely explanation for this is the crack closure phenomenon reported by Elber [3] and caused by crack wake plasticity.

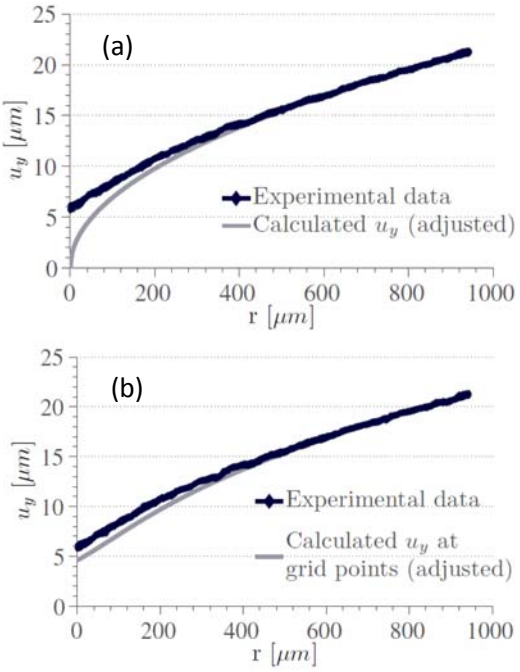

Figure 4. Typical results from constant amplitude loading: (a) fitted with equation (3); (b) fitted with the full equation (2) [6]

2.2. Pommier and Hamam Model

Pommier and Hamam [10] noted that crack tip plasticity will cause additional displacement, which may not be well modelled by the Westergaard elastic solution [9]. They therefore proposed that the full solution for the crack tip displacement field may be thought of as the superposition of elastic and plastic terms. The full approach requires comparison between an elastic-plastic finite element model and the elastic crack solution. By subtracting the latter, one obtains the contribution of the plasticity alone. However, close to the crack tip, one can simplify the relative displacements along the crack flanks as

$$u_y = \frac{8K_I}{E}\sqrt{\frac{r}{2\pi}} + \rho \quad (4)$$

where ρ is a 'plastic intensity factor' with units of length. Of course, there is no singularity involved with this term, so the term may be somewhat misleading. Further, we will note that when $r = 0$ then equation (4) gives simply

$$u_y = \rho \quad (5)$$

which shows that with the approximate elastic and plastic fields used here that ρ is simply equal to the crack tip opening displacement. Pommier and Hamam argue that a significant cyclic variation in ρ is required for fatigue crack propagation and that this may explain the fatigue crack growth threshold.

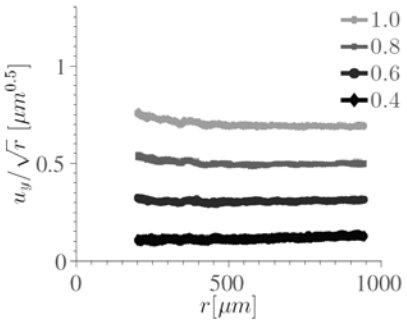

Figure 5. Results from Figure 4, replotted as normalised displacement against distance from the crack tip at different values of P/P_{max}

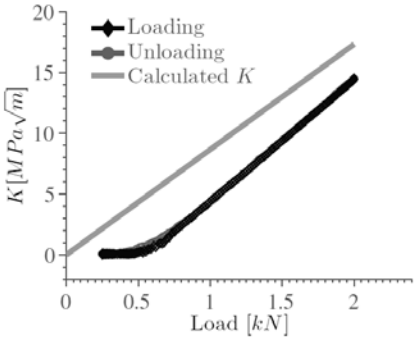

Figure 6. Variation of stress intensity factor with load: results extracted from Figure 4.

By plotting the relative displacement against $\sqrt{r}$, one can use equation (4) to obtain K from the slope and ρ from the intercept. The results may be plotted in K - ρ space, as shown in Figure 7. It may readily be seen that this gives a hysteresis loop, which is broadly of the same shape as predicted in [10].

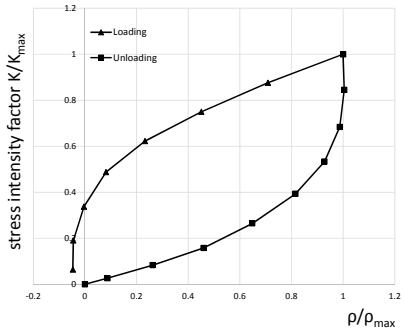

Figure 7. Variation of normalised K and ρ during one cycle of loading, plotted in K - ρ space as suggested in [10]

2.2. The CJP model

The final model that we shall explore is that proposed by Christopher, James, and Patterson [11]. The authors' idea is to capture the effects of the plastic zone ahead of the crack and the plastic wake by means of suitable modifications to the *elastic* stress field. This is achieved by considering the interaction forces between a plastic enclave and the surrounding elastic material. Figure 8 shows a schematic of the model.

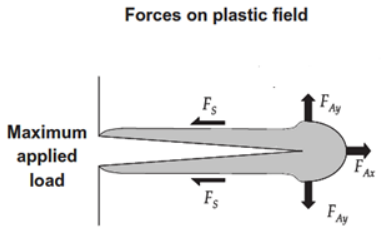

Figure 8:Diagram showing the interaction forces between the plastic enclave and the surrounding elastic material (after [11]).

In the original CJP paper, the approach is shown to lead to four parameters: the Forward Stress Intensity Factor, K_f; the contribution due to shielding, K_r; a shear stress intensity factor K_s; and the bounded T-stress. Of these, the first two would seem to be the dominant terms, with the first representing the applied crack tip driving force and the second the contribution due to material response (i.e. closure and/or crack tip shielding by residual stress). Vasco-Olmo [12] has evaluated the two contributions using a digital image correlation procedure and an Al 4%Cu alloy, very similar to that used here. A typical set of his results is shown in Figure 9.

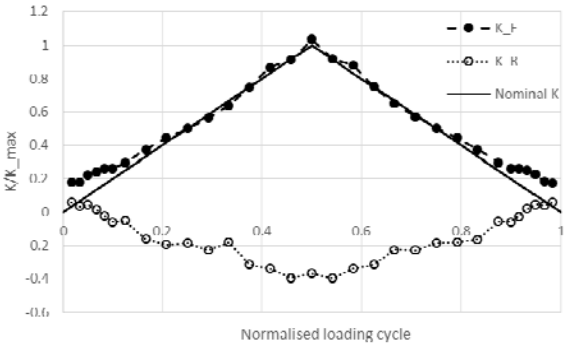

Figure 9: Results obtained by Vasco Olmo, [12], showing the variation of K_F and K_R through a load/unload cycle for an Al 4%Cu CT specimen.

It will be seen from Figure 9 that the K_r term is negative for most of the cycle. Of course, there is no singularity if the crack tip is loaded in compression, and a net negative stress intensity factor makes no physical sense. Hence, Nowell et al. [13] have argued that the appropriate parameter to consider is the net stress intensity (K_r + K_r). When this is considered, the data shown in Figure 9 may be re-plotted and compared with O'Connor's data [6], obtained with the same material, but in an entirely independent experiment. This comparison is shown in Figure 10, after adjusting for the different reference image used in each experiment. The comparison between the two sets of data is striking, and it will be seen that the shielding effect is very significant. The stress intensity factor remains at its minimum value until about 20% of the way through the load cycle. It then increases at approximately the same rate as predicted by

the nominal elastic solution, eventually reaching half the nominal value at maximum load.

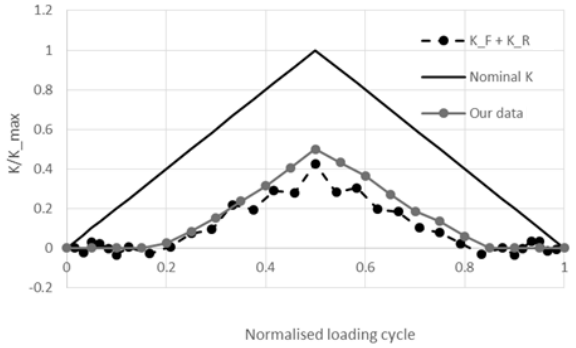

Figure 10: Vasco Olmo's data [12] plotted as delta K against loading cycle and compared against O'Connor's results [6]

DISCUSSION AND CONCLUSIONS

The results shown above show that crack face deformations are quite close to those predicted elastically, but with an offset due to crack tip shielding. Whilst detailed information can be obtained using DIC at a range of length scales, the principal weakness of the method is that it is a surface measurement only. Conditions where the crack front breaks a free surface are very different from at the tip of a crack within the body of the material. In the latter case, conditions of plane strain must almost certainly prevail. Hence, the real challenge, if we are to understand fatigue crack propagation better is to obtain similar data remote from the surface. Here, X-Ray tomography combined with digital volume correlation offers some promise, but it has so far proved difficult to get appropriate features for tracking using mainstream engineering alloys of interest. Further, penetration of the X-rays is very limited, unless a synchrotron source is used, so that experiments reported so far tend to be on very small specimens. Nevertheless, it is clearly necessary to obtain such data if future progress is to be made.

ACKNOWLEDGEMENTS

The authors would like to thank Mr Sam O'Connor, and Dr Kalin Dragnevski, who carried out some of the experimental work described here. They would also like to thank Dr Jose Manuel Vasco Olmo for providing the original data from Figure 9 to enable comparison.

REFERENCES

[1] S. Nishida, Failure Analysis in Engineering Applications, Butterworth-Heinemann, Oxford, 1992.

[2] P. Paris and F. Erdogan, A critical analysis of crack propagation laws, *Trans. ASME: Journal of Basic Engineering*, 528-534, 1963.

[3] W. Elber, Fatigue crack closure under cyclic tension, *Engineering Fracture Mechanics*, **2**, 37–45, 1970.

[4] A.K. Vasudevan K., Sadananda K, and N. Louat, Two critical stress intensities for threshold crack propagation. *Scripta Mettallurgica et Materialia*, **28**, 65-70, 1993.

[5] P.F.P. de Matos, P.F.P., and D. Nowell, Experimental and numerical investigation of thickness effects in plasticity-induced fatigue crack closure, *Int. Jnl Fatigue*, **31**, 1795-1804, 2009.

[6] S.J. O'Connor, Plasticity-induced fatigue crack closure: an investigation using digital image correlation, MSc Thesis, University of Oxford, 2015.

[7] J.M. Vasco-Olmo and F.A. Díaz, Experimental evaluation of plasticity-induced crack shielding from isochromatic data, *Optical Engineering*, **54(8)**, 081203, 2015.

[8] P. Lopez-Crespo, A. Shterenlikht, E.A. Patterson, J.R. Yates, and P.J.Withers, The stress intensity of mixed mode cracks determined by digital image correlation, *Journal of Strain Analysis*, **43(8)**, 769-780, 2008.

[9] H.M. Westergaard, Bearing Pressures and Cracks, *Journal of Applied Mechanics*, **6**, A49-53, 1939.

[10] S. Pommier and R. Hamam, Incremental model for fatigue crack growth based on a displacement partitioning hypothesis of mode I elastic□plastic displacement fields, *Fatigue & Fracture of Engineering Materials & Structures*, **30(7)**, 582-598, 2007.

[11] C.J., Christopher, M.N. James, E.A. Patterson and K.F. Tee, Towards a new model of crack tip stress fields, *International Journal of Fracture*, **148**, 361-, 2007.

[12] J.M. Vasco-Olmo, Experimental evaluation of plasticity induced crack shielding effect using full-field optical techniques for stress and strain measurement, PhD thesis, University of Jaén, 2014.

[13] D. Nowell, K. Dragnevski, and S.J. O'Connor, Investigation of Fatigue Crack Models by Micro-scale Measurement of Crack Tip Deformation, *Int Jnl Fatigue,* In Press, 2018.